Theoretical study of Auger recombination in a GaInNAs 1.3 μm quantum well laser structure

A. D. Andreev
Department of Physics, University of Surrey, Guildford GU2 7XH, United Kingdom

E. P. O'Reilly
NMRC, University College, Lee Maltings, Prospect Row, Cork, Ireland

(Received 18 August 2003; accepted 7 January 2004)

We present a theoretical study of Auger recombination processes in a GaInNAs/GaAs quantum well structure designed for 1.3 μm laser emission. The calculations are based on a 10×10 **k·p** model, incorporating valence, conduction, and nitrogen-induced bands. The Auger transition matrix elements are calculated explicitly, without introducing any further approximations into the Hamiltonian used. We consider two main Auger recombination channels: the process when the energy released from the electron-hole recombination causes electron excitation (CHCC process) and the process with hole excitation to the split-off valence band (CHHS process). The CHHS process is shown to be dominant. Good agreement is found when comparing the calculated Auger rates with experimental values of the Auger contribution to the threshold current of GaInNAs quantum well lasers. © *2004 American Institute of Physics.* [DOI: 10.1063/1.1664033]

The material system, GaInNAs, is of significant interest, both because it provides a route to 1.3 μm vertical cavity lasers,[1,2] and also because it potentially enables a reduced temperature sensitivity of the threshold current compared to conventional InP-based 1.3 μm lasers. It is now well established that nonradiative recombination crucially influences the performance of InP-based lasers.[3] The main mechanism of nonradiative recombination is Auger recombination (AR).[1] Recent experimental analysis estimates that AR contributes 30%–50% of the total threshold current both in GaInNAs and in InP-based 1.3 μm devices at room temperature.[4,5] AR is then the main cause of the rapid increase in threshold current at room temperature and above.

The aim of this letter is to study theoretically the AR rate and its temperature dependence in GaInNAs quantum wells (QWs). We consider the most likely AR paths, and identify hole excitation as the dominant AR process. We show that the Auger recombination coefficient has a relatively weak (nearly linear) temperature dependence in the QW considered, but conclude that AR will dominate the high-temperature threshold characteristics of ideal GaInNAs lasers.

Although AR rates have been calculated previously by many authors,[6–15] the results presented here are the most advanced to date for lasers operating in the telecomm (1.3–1.5 μm) waveband. In narrow-gap materials, the spin-orbit splitting is larger than the band gap and therefore the mechanism of Auger recombination in such materials is different from that in the 1.3 μm structure.[5] Considerable progress has been made in the development of accurate Auger calculations for narrow-gap materials;[6–11] by contrast, a variety of severe assumptions and approximations have been made in previous calculations of the AR rate for 1.3–1.5 μm QW structures. For example, in Ref. 12, the spin–orbit interaction was neglected and only the CHCC process was considered (see Fig. 1). A linear approximation was used for the electron-hole overlap integral in Ref. 13; the effect of QW strain was omitted in Refs. 12 and 14; and the effect of light-heavy hole mixing was neglected in Ref. 14; while a simple effective-mass approximation was used to calculate the overlap integrals in Ref. 15. All of these approximations can lead to errors of up to one order of magnitude in the calculated AR rate, and they also obscure trends in the dependence of AR rate on temperature and structure parameters.

For our calculations we consider a 64 Å $Ga_{0.64}In_{0.36}N_{0.017}As_{0.983}/GaAs$ QW structure, similar to that used as the active region of a 1.3 μm laser whose experimental characteristics have recently been studied in detail.[5] The conventional eight-band **k·p** Hamiltonian must be extended to a ten-band model[16] to describe the band structure of GaInNAs, adding two (spin-degenerate) nitrogen-related bands to the usual two conduction and six valence band Bloch functions.[17] The 10×10 **k·p** model has been successfully used to describe the energy spectra and optical transitions in GaInNAs QWs,[18] and to describe the gain spectra as a function of carrier density in 1.3 μm laser structures.[19] Calculation of the Auger rates requires several stages: first, determination of the QW band structure and wave functions, including highly excited states; then evaluation of the overlap integrals and Coulomb matrix elements; and finally the summation over all initial and final carrier states for the dif-

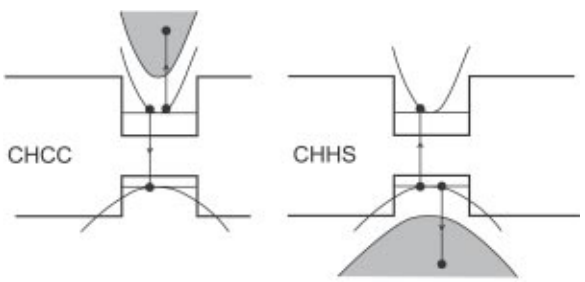

FIG. 1. Schematic diagram of the two major Auger processes in a GaInNAs QW: (a) the CHCC process with electron excitation; (b) the CHHS process with hole excitation into the spin–split–off band. The shaded areas designate unbound electron or hole states.

ferent processes considered. Auger processes are commonly classified by labeling the initial and final states with letters describing whether the carriers are in the conduction (C), heavy-hole (H), or spin-split-off (S) bands. Figure 1 shows the band diagram corresponding to the two major Auger proceses, CHCC and CHHS. In quantum wells, heavy- and light-hole states are mixed at nonzero in-plane momentum; therefore "H" stands both for light and heavy holes in the Auger process classification. In addition, the excited state in a QW structure may be either bound (a confined QW state with large in-plane momentum) or unbound. In the GaInNAs structure studied here, the Auger process with electron excitation to a bound state turns out to be negligible (partly due to the presence of the nitrogen band); the excitation of a hole to a bound state is also not important, due to the large in-plane momentum required. Auger processes involving phonons are generally not important for the relatively high ($T>250$ K) temperatures considered here. As a result only the two Auger processes depicted in Fig. 1 are significant in the GaInNAs QW studied. In both these processes the final state for the excited carrier is unbound.

The calculated energy spectra of carriers localized in the given GaInNAs QW structure can be found in Refs. 5 and 20. For the excited carrier states we note that above-barrier reflection at the QW boundaries must be taken into account (i.e., the wave function of the excited state is *not* just a plane wave, see below).

The Coulomb matrix element M for the Auger recombination process in the QW is $M=M_I-M_{II}$; with M_I given by[8,9]

$$M_I=\int \frac{dq}{(2\pi)} \frac{I_{13}(q)I_{24}(-q)}{[q^2+(k_{1\|}-k_{3\|})^2]\kappa(q,\omega)}, \qquad (1)$$

where $I_{\alpha\beta}(q)=\int \Psi^*_\alpha(x,k_{\alpha\|})\Psi_\beta(x,k_{\beta\|})e^{iqx}dx$ is the overlap integral between the states with indices α and β (equal to 1, 2, 3, and 4 denoting the states of the four carriers involved in the Auger process); the x axis is directed along the QW growth direction; $\kappa(q,\omega)$ is the dielectric function determined using the Lindhard formula,[21] q is the momentum transferred, and $\hbar\omega$ the energy transferred during the Auger process; $k_{i\|}$ is the in-plane momentum of the ith state. M_{II} is obtained from M_I by formal $3\leftrightarrow4$ substitution. It is important to calculate the overlap integral using the wave functions determined from the multiband model; the product $\Psi_\alpha\Psi_\beta$ in the above expression for the overlap integral involves the scalar product of two vectors (in the basis of the ten Bloch functions). This scalar product strongly depends on the in-plane momentum of the particles.

It follows from Eq. (1) that the Auger matrix elements are determined from two overlap integrals: an electron-hole overlap integral between two states localized in the QW and an overlap integral between a localized state and a highly excited unbound state. We describe briefly the main characteristics of these two important quantities. The solid line in Fig. 2 shows the dependence of the electron-hole overlap integral I_{eh} on the momentum transferred. The dependence $I_{eh}(q)$ is nonlinear, so that the previously used linear approximation[13] for $I_{eh}(q)$ is generally not valid for QW structures. It follows from an analysis of Eq. (1) that the matrix element consists mainly of two contributions:[8,9] a contribution from an area where "small" values of momentum are transferred, $q\sim|k_{e\|}-k_{h\|}|<\pi/a$ (a is the QW width); and a contribution where "large" values of momentum are transferred, $q\sim k_g$, where k_g satisfies the equation $\hbar^2k_g^2/(2m_c)=E_g$ (E_g is the effective band gap, m_c is the effective electron mass). In practice the existence of these two contributions means that the whole range of q values is important in Eq. (1), from very small values (where I_{eh} varies linearly with q) to relatively large values of q (where the linear approximation used in Ref. 14 is in error by more than one order of magnitude). The value of the I_{eh} overlap integral is also strongly influenced by the light-heavy hole mixture at nonzero in-plane momentum. It should be noted that the electron-hole overlap integral is dependent on various QW parameters, including the quantum well width and depth, the strain, and the effective band gap; this can give a strong dependence of the Auger rate on these structure parameters.[11] To study the influence of the N band on the electron-hole overlap integral we also considered an artificial N-free InGaAs-like QW structure with the same effective band gap and band offsets (details of this structure are given in Ref. 20). The overlap integral for this artificial structure is shown by the dashed line in Fig. 2. The interaction with the N band reduces the conduction band (s like) component of the electron wave function, while the hole states are largely unaffected by the presence of the N band. The change in the electron wave function leads to a small reduction in the overlap integral at a given q value compared to the N-free structure. Thus, the presence of nitrogen leads to a decrease in I_{eh}; this decrease is larger for larger N content x_N (if the band gap and other structure parameters are kept unchanged). The Auger matrix element depends also on the overlap integral I_{ex} between the localized and excited (electron or hole) states. From a mathematical point of view, this is an integral between the "smooth" wave function of a carrier localized in the QW (with wave vector $k\sim\pi/a$) and the highly oscillating wave function of an excited carrier (with wave vector $k\sim k_g$). As a consequence, the overlap integral I_{ex} is usually small compared to I_{eh}. Deviation of the excited state wave function from a simple plane wave also significantly influences the value of I_{ex}.

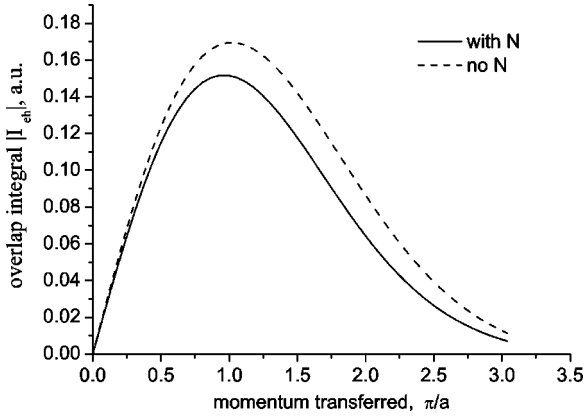

FIG. 2. Electron-hole overlap integral versus transferred momentum $q=k_{e\|}$-$k_{h\|}$, in units of π/a where $a=64$ Å is the QW width. The curves are for the case when $k_{h\|}=0$ and $k_{e\|}$ is varied; the case when $k_{h\|}$ is varied and $k_{e\|}$ is fixed give a very similar variation of $I_{eh}(q)$. Solid lines and dashed lines: GaInNAs and artificial QW, respectively.

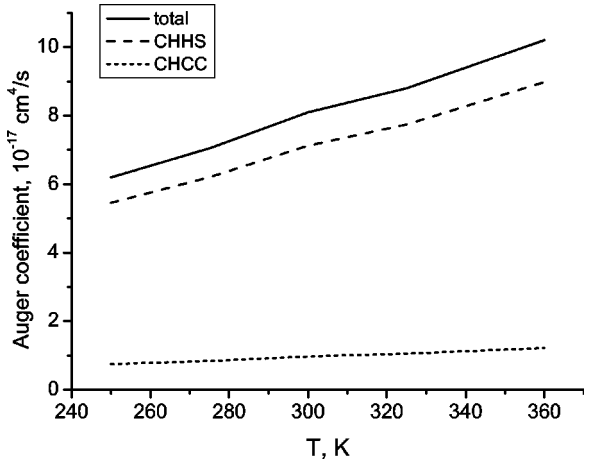

FIG. 3. Calculated Auger recombination coefficient vs temperature for a GaInNAs QW with the same parameters as in Fig. 2. Solid line: total Auger coefficient; dashed and dotted lines: contributions from the CHHS and CHCC processes, respectively. Electron and hole densities are 10^{12} cm^{-2}.

The AR rate is calculated by summing over all possible initial and final states using Fermi's golden rule. Mathematically this requires the calculation of a five-dimensional integral over the carrier momentum components and a summation over the electron and hole QW levels (these final integrals were calculated numerically). Figure 3 shows the calculated AR coefficient C as a function of temperature. The value of C calculated is about 5% smaller than the value we obtain for the equivalent artificial N-free structure. We define this coefficient as $C=G/n^3$, where G is the Auger rate calculated for a carrier density of $n=p=10^{12}$ cm^{-2}. The Auger coefficient (and its temperature dependence determined in this way) does depend on the carrier density; the calculated AR rate has a slightly subcubic dependence on carrier density. It follows from Fig. 3 that the main AR path is via the CHHS recombination process. This result agrees with a previous experimental and theoretical analysis, which concluded that the CHHS process dominates in InGaAs(P)-based devices.[22] The calculated AR coefficient depends weakly on temperature, because Auger recombination is a thresholdless process in QW heterostructures, due to the lack of momentum conservation along the QW growth direction.[8,12,23] Previous experimental measurements also confirmed a weak temperature dependence of the Auger coefficient in an InGaAsP-based QW structure.[24] The temperature dependence of the Auger contribution J_A to the total laser threshold current is then dominated by the variation of the threshold carrier density with temperature, $n_{\mathrm{th}}(T)$. Combining the AR results presented in this letter with a detailed calculation of $n_{\mathrm{th}}(T)$,[25] we find very good agreement between the calculated values of $J_A(T)$ and the experimentally determined values.[5] For example at $T=300$ K the calculated $J_A=205$ A/cm^2, and the experimental value $J_A^{(\mathrm{exper})}=177$ A/cm^2; at $T=360$ K the calculated $J_A=1045$ A/cm^2 and the experimental $J_A^{(\mathrm{exper})}=1076$ A/cm^2.

In summary, we have studied theoretically the role of Auger recombination in a GaInNAs/GaAs strained QW. We found CHHS recombination to be the dominant Auger recombination path, involving hole excitation to an unbound state in the spin-split-off band. The calculated AR coefficient in GaInNAs QWs is of the same order of magnitude as in nitrogen-free structures with similar parameters (same effective band gap and band offsets). The introduction of nitrogen decreases the electron-hole overlap integral, but also leads to an increased conduction band density of states; the combination of these two factors results in an approximately unchanged AR coefficient, C. We conclude that Auger recombination plays an important role at room temperature and above in GaInNAs 1.3 μm QW laser structures, putting an intrinsic limit on the temperature stability of the threshold characteristics. The AR rate is sensitive to the variation of QW structure parameters (e.g., strain, effective barrier height and band gap), so further investigations would be valuable to identify optimized device structures. Overall, our results confirm that the intrinsic gain and loss characteristics of GaInNAs make this material very attractive for vertical cavity lasers and other integrated GaAs-based devices.

This work was supported by Science Foundation Ireland.

[1] M. Weyers, M. Sato, and H. Ando, Jpn. J. Appl. Phys., Part 2 **31**, L853 (1992).
[2] K. D. Choquette *et al.*, Electron. Lett. **36**, 1388 (2000).
[3] A. Sugimura, IEEE J. Quantum Electron. **QE-17**, 627 (1981); T. Higashi, S. J. Sweeney, A. F. Phillips, A. R. Adams, E. P. O'Reilly, T. Uchida, and T. Fujii, IEEE J. Sel. Top. Quantum Electron. **5**, 413 (1999).
[4] S. J. Sweeney, T. Higashi, A. D. Andreev, A. R. Adams, T. Uchida, and T. Fujii, Phys. Status Solidi B **223**, 573 (2001).
[5] R. Fehse, S. Tomic, A. R. Adams, S. J. Sweeney, E. P. O'Reilly, A. D. Andreev, and H. Riechert, IEEE J. Sel. Top. Quantum Electron. **8**, 801 (2002).
[6] M. E. Flatte, C. H. Grein, T. C. Hasenberg, S. A. Anson, D. J. Jang, J. T. Olesberg, and T. F. Boggess, Phys. Rev. B **59**, 5745 (1999); D. J. Jang, M. E. Flatte, C. H. Grein, J. T. Olesberg, T. C. Hasenberg, and T. F. Boggess, Phys. Rev. B **58**, 13047 (1998); C. H. Grein, M. E. Flatte, J. T. Olesberg, S. A. Anson, L. Zhang, and T. F. Boggess, J. Appl. Phys. **92**, 7311 (2002).
[7] B. Vinter, Phys. Rev. B **66**, 045324 (2002).
[8] A. D. Andreev, Mater. Res. Soc. Symp. Proc. **484**, 117 (1998).
[9] A. D. Andreev and G. G. Zegrya, Appl. Phys. Lett. **70**, 601 (1997).
[10] A. D. Andreev and D. V. Donetsky, Appl. Phys. Lett. **74**, 2743 (1999).
[11] A. D. Andreev, E. P. O'Reilly, A. R. Adams, and T. Ashley, Appl. Phys. Lett. **78**, 2640 (2001).
[12] M. I. Dyakonov, and V. Yu. Kachorovskii, Phys. Rev. B **49**, 17130 (1994).
[13] J. Wang, P. Allmen, J.-P. Leburton, and K. J. Linden, IEEE J. Quantum Electron. **31**, 364 (1995).
[14] A. S. Polkovnikov and G. G. Zegrya, Phys. Rev. B **58**, 4039 (1998); N. A. Gun'ko, A. S. Polkovnikov, and G. G. Zegrya, Semiconductors **34**, 448 (2000).
[15] O. Gilard, F. Lorez-Dupuy, G. Vassilieff, S. Bonnefont, P. Arguel, J. Barrau, and P. Le Jeune, J. Appl. Phys. **86**, 6425 (1999).
[16] E. P. O'Reilly, A. Lindsay, S. Tomic, and M. Kamal-Saadi, Semicond. Sci. Technol. **17**, 870 (2002).
[17] T. B. Bahder, Phys. Rev. B **41**, 11992 (1990); **46**, 9913 (1992).
[18] S. A. Choulis, T. J. C. Hosea, S. Tomic, M. Kamal-Saadi, A. R. Adams, E. P. O'Reilly, B. A. Weinstein, and P. J. Klar, Phys. Rev. B **66**, 165321 (2002).
[19] M. Hofmann *et al.*, IEEE J. Quantum Electron. **38**, 213 (2002).
[20] S. Tomic and E. P. O 'Reilly, Physica E (Amsterdam) **13**, 1102 (2002).
[21] W. W. Chow and S. W. Koch, *Semiconductor-Laser Fundamentals* (Springer, Berlin, 1999).
[22] S. J. Sweeney, A. R. Adams, M. Silver, E. P. O'Reilly, J. R. Watling, A. B. Walker, and P. J. A. Thijs, Phys. Status Solidi B **211**, 525 (1999).
[23] G. G. Zegrya and V. A. Kharchenko, Sov. Phys. JETP **74**, 173 (1992).
[24] G. Fuchs, C. Schiedel, A. Hangleiter, V. Härle, and F. Scholz, Appl. Phys. Lett. **62**, 396 (1993).
[25] A. D. Andreev and E. P. O'Reilly (unpublished).